LFA-1-induced T cell migration on ICAM-1 involves regulation of MLCK-mediated attachment and ROCK-dependent detachment

Andrew Smith*, Madelon Bracke*,‡, Birgit Leitinger§, Joanna C. Porter¶ and Nancy Hogg**

Leukocyte Adhesion Laboratory, Cancer Research UK London Research Institute, Lincoln's Inn Fields Laboratories, Lincoln's Inn Fields, London WC2A 3PX, UK

*These authors contributed equally to this work
‡Present address: Department Pharmacoepidemiology and Pharmacotherapy, Utrecht Institute for Pharmaceutical Sciences, PO Box 80082, 3508 TB Utrecht, The Netherlands
§Present address: Sackler Institute for Muscular Skeletal Research, Department of Medicine, University College London, 5 University Street, London WC1E 6JJ, UK
¶Present address: MRC Laboratory for Molecular Cell Biology, University College London, Gordon Street, London WC1E 6BT, UK
**Author for correspondence (e-mail: nancy.hogg@cancer.org.uk)

Accepted 9 April 2003
Journal of Cell Science 116, 3123-3133 © 2003 The Company of Biologists Ltd
doi:10.1242/jcs.00606

Summary

This study analyzes signaling events initiated through binding of the leukocyte integrin LFA-1 to ICAM-1, which leads to T cell attachment, polarization and random migration. These events are critically dependent on dynamic changes in the acto-myosin cytoskeleton under the regulation of myosin light chain kinase and ROCK (Rho kinase). A key finding is that the activity of these two kinases is spatially segregated. Myosin light chain kinase (MLCK) must operate at the leading edge of the T cell because blocking its activity causes the polarized T cell to retract from the front of the cell. These activities are mirrored by inhibiting calmodulin, the activator of MLCK. In contrast inhibition of ROCK (and RhoA) has the effect of preventing detachment of the T cell trailing edge, showing that this kinase operates at the rear of the cell. This compartmentalized activity of the two kinases is reflected in their localization within the T cell. Myosin light chain kinase is concentrated at the leading edge, overlapping F-actin, whereas ROCK is more widely distributed in the trailing edge of the T cell. Thus these two kinases perform two different functions in the migrating T cell, with myosin light chain kinase activity important for attachment and movement at the leading edge and ROCK activity required for the detachment of the trailing edge. These two acto-myosin-dependent processes operate coordinately to cause forward migration of a T cell.

Supplementary figure and movies available online

Key words: T lymphocyte, LFA-1, Migration, MLCK, Rho kinase

Introduction

The ability of T cells to adhere and migrate is critical for a fully functional immune system. In response to inflammatory signals, T cells leave the blood stream by migrating along vascular endothelial surfaces, scanning for a suitable exit point into the tissue (reviewed in Serrador et al., 1999; Worthylake and Burridge, 2001). In vitro T cells are observed to move across the surfaces of antigen presenting cells in a state of constant motility (Friedl and Gunzer, 2001), and T cells deep within lymph nodes are highly motile, as demonstrated by two photon microscopy (Miller et al., 2003). Therefore, persistent migration is central to T cell function, and it is important to understand the molecular mechanisms that underlie this motility.

LFA-1 is abundantly expressed by leukocytes and is the main receptor used by T cells for adhesion via the ICAM family of ligands. The ability of LFA-1 to act as a signaling receptor has not been extensively examined, as it has been chiefly associated with promoting cell-cell contact, thereby optimizing signaling through other receptors. Clustering of LFA-1 and an increase in affinity for ICAM-1, resulting from a conformational alteration in the integrin ectodomain, promote LFA-1-mediated adhesion (Stewart and Hogg, 1996; van Kooyk and Figdor, 2000). These changes are achieved via intracellular signals generated through engagement of other cell surface receptors. However, LFA-1 can also be triggered directly through the use of stimulatory anti-LFA-1 antibodies or by exposure to ICAM-1 together with divalent cations Mg^{2+} or Mn^{2+} (Stewart and Hogg, 1996). This method of activation bypasses the need for inside out signaling and allows the analysis of LFA-1 signaling, initiated by ICAM-1 binding, in isolation from other cell surface receptors.

Cells move by coordinating the generation of lamellipodial protrusions at the front of the cell leading to new attachments, followed by the detachment of previous adhesions at the rear of the cell (Horwitz and Parsons, 1999). LFA-1 is directly involved in promoting cell contact as T cell attachment to ICAM-1 is dependent upon the ability of LFA-1 to signal remodeling of the actin cytoskeleton (Porter et al., 2002). LFA-1 is also involved in generating signals, such as PKC-β1-dependent microtubule rearrangements, that allow adhesion to be translated into migration (Volkov et al., 2001). Here we describe how LFA-1 induces myosin motor activity through the activation of two kinases, myosin light chain kinase (MLCK) and ROCK. The location and activity of both kinases within the cell is restricted, with MLCK at the leading edge and ROCK concentrated at the trailing edge of the cell.

Materials and Methods

Inhibitors, antibodies and other reagents

The pharmacological inhibitors ML-7 (MLCK), Y-27632 (ROCK), W-7 [calmodulin (CaM)] and C3 exoenzyme (RhoA GTPase) were purchased from Merck Biosciences Ltd (Nottingham, UK); 2,3-butanedione monoxime (BDM) (myosin ATPase) was from Sigma-Aldrich (Poole, UK); and Alexa 546-phalloidin and Alexa 488-phalloidin were from Cambridge Bioscience (Cambridge, UK). The following antibodies were used: MLCK mAb K36 (Sigma); ROCK-I (BD Biosciences, Oxford, UK); rabbit anti-myosin II (Biomedical Technologies Inc, Stoughton, MA, USA); Alexa 488-goat anti-rabbit IgG (Cambridge Bioscience) and Alexa 488-rabbit anti-mouse IgG (Cambridge Bioscience).

ICAM-1Fc was produced as a chimeric protein, consisting of the five extracellular domains of ICAM-1 fused to the Fc fragment of human IgG1 (Berendt et al., 1992). The fluorescent cell label 2′,7′-bis-(carboxyethyl)-5(6′)-carboxyfluorescein (BCECF-AM) was purchased from Calbiochem.

The following peptides linked to biotinylated antennapedia peptide were synthesized by the Protein and Peptide Chemistry Laboratory of the Cancer Research UK London Research Institute: MLCK autoinhibitory or LSM1 sequence (LSKDRMKKYMARR) (Tanaka et al., 1995; Walker et al., 1998), a scrambled version of the LSM1 peptide with Tyr altered to Ala (RSKDMRAKAKARL) and biotinylated antennapedia peptide alone.

Cell attachment assays

Peripheral blood mononuclear cells were prepared from single donor leukocyte buffy coats and T cells expanded in culture as previously described (Porter and Hogg, 1997). Before use, T cells were washed three times in HEPES buffer (20 mM HEPES, 140 mM NaCl, 2 mg/ml glucose, pH 7.4) and labelled with 2.5 μM BCECF-AM in the same buffer for 30 minutes at 37°C followed by two further washes. Flat-bottomed Immulon-1® 96-well plates (Dynatech, Chantilly, VA) were precoated with 50 μl of ICAM-1Fc (3 μg/ml) in PBS overnight at 4°C. The plates were blocked with 2.5% BSA in PBS for 2 hours at room temperature, then washed once with PBS and twice in HEPES buffer. T cells were pre-incubated with inhibitors for 15 minutes (or overnight at 37°C for C3 exoenzyme) following titration to determine the optimal dose. The inhibitors were MLCK inhibitor ML-7, ROCK inhibitor Y-27632 (both 0-200 μM), CaM inhibitor W-7 (0-100 μM) and RhoA GTPase inhibitor C3 exoenzyme (0-20 μg/ml). T cells were preincubated with the antennapedia peptides at concentrations from 0 to 20 μg/ml for 90 minutes at 37°C and washed twice with HEPES buffer before use in the experiment. T cells at 2×10^5 cells/well were added to 96-well plates coated with ICAM-1Fc and treated with HEPES buffer containing 5 mM Mg^{2+}/1 mM EGTA (Mg^{2+}/EGTA buffer). The T cells were centrifuged at 100 ***g*** for 1 minute, prior to 40 minutes of incubation at 37°C. Non-adherent cells were removed by washing three times in warmed Mg^{2+}/EGTA buffer (150 μl/well). T cell attachment was quantified using a Cytofluor multiwell platereader (PerSeptive Biosystems, Hertford, UK).

Western blotting

T cells were suspended at 5×10^7/ml in ice cold lysis buffer [50 mM Tris pH 8 containing 150 mM NaCl, 2 mM $MgCl_2$, 2 mM EGTA, 1% Triton X-100, 10 μg/ml phenylmethylsulphonyl fluoride and Complete™ protein inhibitor cocktail (Roche Diagnostics, Lewes, UK) used according to the manufacturer's instructions] and lysed for 20 minutes on ice. The lysate was microfuged for 15 minutes to remove insoluble material. Proteins were separated by SDS-PAGE. After transfer to nitrocellulose membrane and incubation with primary antibodies, the bound antibody was detected with HRP-conjugated sheep anti-mouse Ig (Amersham Biosciences UK Ltd, Chalfont St Giles, UK) and ECL western blotting detection reagents (Amersham Biosciences UK Ltd).

Confocal microscopy

13 mm round glass coverslips were precoated with 300 μl ICAM-1Fc (3 μg/ml) in PBS overnight at 4°C. Coverslips were blocked with 2.5% BSA in PBS for 2 hours at RT and then washed three times with PBS and once with HEPES buffer at 4°C. T cells were washed three times in HEPES buffer before being added to the coverslips (2×10^5 cells/coverslip) in 100 μl of Mg^{2+}/EGTA buffer. Cells were incubated for 10 minutes on ice and then a further 30 minutes at 37°C. Unbound cells were removed with four gentle washes with Mg^{2+}/EGTA buffer. Adherent cells were then fixed with 3% formaldehyde in PBS for 20 minutes at room temperature. After two washes with PBS, cells were permeabilized with 0.1% Triton-X-100 for 5 minutes on ice in order to stain for intracellular proteins. Cover slips were incubated with MLCK mAb (1:100), ROCK I mAb (2.5 μg/ml), and respective ascites and IgG1 isotype controls or rabbit anti-myosin II (1:100) for 30 minutes at RT, then followed by Alexa 488-goat anti-mouse IgG (1:200), goat anti-rabbit IgG (1:200) and 2.5 units/ml Alexa 546-phalloidin for 30 minutes at RT. The images were taken on a Zeiss Laser Scanning Microscope LSM5101.

Detection of cell spread area by laser scanning cytometry

The Laser Scanning Cytometer (CompuCyte, Mass, USA) combines features of both flow and image cytometers in that it measures fluorescence and light scatter from immobilized cells that are moved through a 488 nm laser line on a motorized stage (Darzynkiewicz et al., 1999). The spread contours of T cells, mounted on ICAM-1-coated coverslips as for confocal microscopy, were defined on the basis of their fluorescence as determined by Alexa 488-phalloidin, and the threshold level was optimized so that as many single cells as possible could be contoured without losing fluorescence information. For each cell, the 'spread area' represents the physical area in μm^2. 6,000 cells were measured per coverslip. The data were analyzed using the unpaired Student's *t*-test, and a value of $P<0.01$ was taken as significant.

Video microscopy

For video-microscopy, 35 mm glass bottom microwell dishes (MatTek Corp., Ashland, Mass, USA) were coated at 4°C overnight with 200 μl of ICAM-1Fc (3 μg/ml) in PBS, then blocked with 2.5% BSA in PBS. T cells at 5×10^5 per dish were allowed to migrate for 20 minutes at 37°C before being exposed to either 20-25 μM ML-7, 10-20 μM Y-27632 or 50 μM W-7 for an additional 10-70 minutes. Images were taken at 5 second intervals using a Nikon Diaphot 300 microscope and AQM^{2001} Kinetic Acquisition Manager software (Kinetic Imaging Ltd., Bromborough, UK). Over a 70 minute period, cells were tracked using Motion Analysis software (Kinetic Imaging Ltd.), and the data analyzed using a Mathematica notebook (Wolfram Research Europe Ltd, Long Hanborough, UK) developed by Daniel Zicha (Cancer Research UK, London).

Results

LFA-1-mediated attachment to ICAM-1 requires acto-myosin interactions

To investigate the signals arising from the interaction of LFA-1 with its ligand ICAM-1, primary human T cells were exposed to Mg^{2+}/EGTA and immobilized ICAM-1. This established protocol causes LFA-1-dependent attachment to ICAM-1 and F-actin reorganization (Dransfield et al., 1992; Porter et al., 2002). To explore the details of the signaling pathway(s)

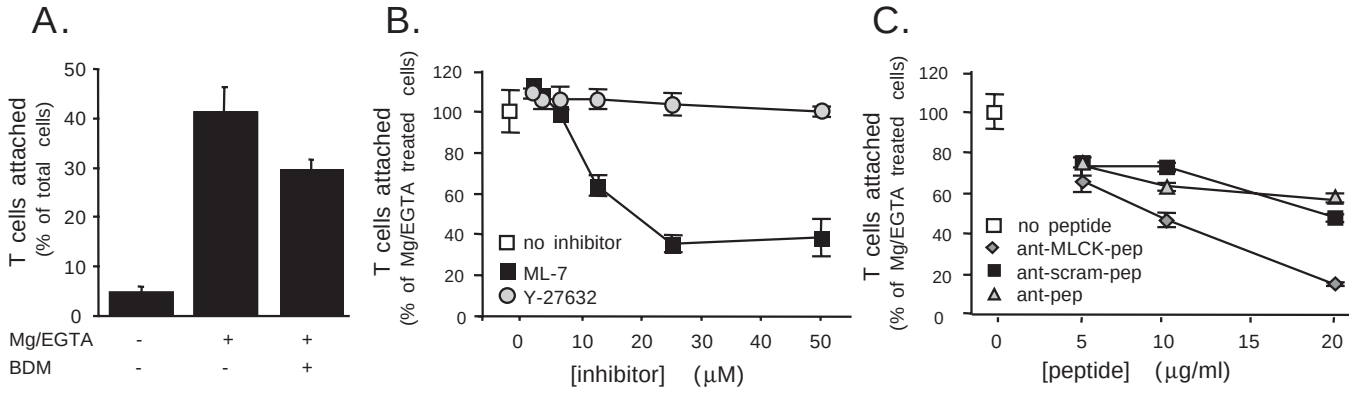

Fig. 1. Inhibition of myosin activation and its effects on LFA-1-mediated T cell attachment to ICAM-1. (A) Attachment of T cells to ICAM-1 with and without Mg^{2+}/EGTA stimulation compared with attachment in the presence of Mg^{2+}/EGTA plus BDM (myosin ATPase inhibitor, 20 mM, n=6, P=0.02). (B) The effect on T cell attachment to ICAM-1 of MLCK inhibitor ML-7 and ROCK inhibitor Y-27632 (0-50 μM). (C) The effect of various peptides on T cell attachment. Antennapedia linked to a 13-mer peptide containing the auto-inhibitory site of MLCK (ant-MLCK-pep), and, as controls, a scrambled version of the same peptide (ant-scram-pep) and antennapedia only (ant-pep) (representative of 5 experiments). Values are expressed in A and B as the mean±s.e.m. and in C as the mean±s.d.

involved in the cytoskeletal reorganization associated with LFA-1-mediated attachment, we used BDM, an inhibitor of the motor protein myosin II. Inhibition of myosin ATPase activity with 20 mM BDM (range of 0-30 mM) significantly decreased T cell binding, providing evidence that T cell adhesion to ICAM-1 requires active myosin (Fig. 1A). Reduced T cell attachment resulting from loss of myosin activity was investigated further by using specific inhibitors.

ML-7 is an inhibitor of MLCK, a serine/threonine kinase that phosphorylates myosin light chains (MLC) promoting acto-myosin contraction (Kamm and Stull, 2001). Titration of ML-7 showed a saturating dose of 25 μM for inhibition of T cell attachment (Fig. 1B). Although ML-7 is an inhibitor of MLCK with a Ki of 300 nM, it can also inhibit protein kinase A (Ki=21 μM) and protein kinase C (Ki=42 μM) (Saitoh et al., 1987). At the concentrations that effectively interfere with attachment, ML-7 is likely to selectively block the activity of MLCK because BIM, a broadly specific PKC inhibitor, had no effect on T cell attachment (data not shown). In order to confirm the specific effect on MLCK, we treated T cells with a 13-mer MLCK auto-inhibitory domain peptide or a scrambled version of the peptide, both of which were fused to antennapedia peptide to promote T cell entry (Tanaka et al., 1995; Walker et al., 1998). The MLCK domain peptide inhibited T cell attachment to ICAM-1 at 10-20 μg/ml (Fig. 1C). The scrambled version of the peptide had a small effect on T cell attachment that was attributable to the antennapedia peptide.

ROCK is another kinase that directly phosphorylates MLC and also indirectly promotes MLC phosphorylation through inhibition of myosin phosphatase (Ishizaki et al., 1996; Kimura et al., 1996). T cell attachment to ICAM-1 was not affected by the ROCK inhibitor, Y-27632 (Fig. 1B). Inhibition by C3 exoenzyme of RhoA, which is the upstream activator of ROCK, similarly had no effect on T cell attachment (see supplementary figure 1, available at jcs.biologists.org/supplemental).

In summary, these data suggest that activation of myosin via MLCK, but not ROCK, has an important role in T cell attachment to ICAM-1.

MLCK and ROCK I expression in T cells

MLCK and ROCK have not previously been identified in T cells. Therefore, confirmation of protein expression was determined by western blot analysis of a T cell lysate. Human MLCK is expressed as a ~130-150 kDa smooth muscle form that is present in most cell types and variants of a larger ~220 kDa non-smooth muscle form (Blue et al., 2002; Kamm and Stull, 2001). Two bands were detected in the T cell lysate, one corresponding to 142 kDa and another at 166 kDa (Fig. 2). As a positive control, the small and large forms of 142 and ~220 kDa, respectively, were observed in murine lung cell lysate using anti-MLCK mAb K36. By comparison with murine lung cells and other cell lines (data not shown), MLCK appears to be expressed in low abundance in human T cells.

T cells contained ROCK I at 160 kDa as detected with anti-ROCK I mAb (Fig. 2). The blots of the T cell and lung lysates were also probed with control ascites or IgG1 mAb and showed no positive labelling (data not shown).

LFA-1-mediated T cell attachment to and migration on ICAM-1

T cells are observed to migrate on ICAM-1-expressing endothelium. We therefore used video microscopy to investigate

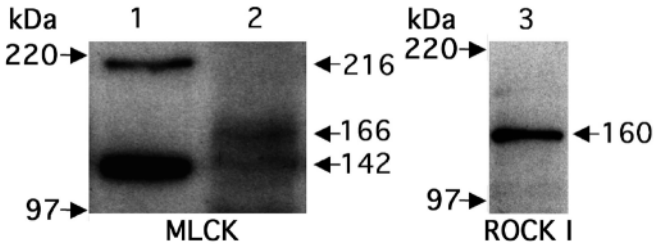

Fig. 2. Identification of MLCK and ROCK in human T cells. Western blot analysis of T cells probed with mAbs specific for MLCK (lane 2) and ROCK I (lane 3). Mouse lung lysate was used as a positive control for the smooth muscle and non-smooth muscle forms of MLCK (lane 1). Molecular weight markers of 220 kDa (myosin) and 97kDa (phosphorylase A) are indicated.

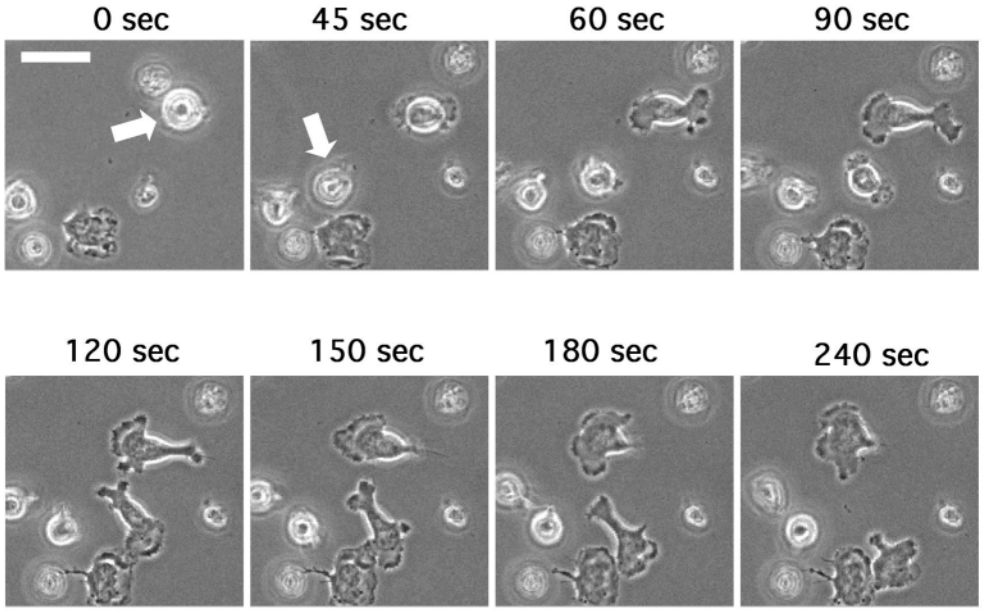

Fig. 3. LFA-1-mediated migration of T cells on ICAM-1. Time lapse video microscopy of human T cells treated with Mg^{2+}/EGTA showing a sequence of initial contact with and migration on ICAM-1. Cells and medium were preheated to 37°C prior to recording. See Movie 1 for further examples of attachment, polarization and migration. The white arrows at time 0 and 45 seconds highlight the cells that have made initial contact with ICAM-1. Bar, 20 μm.

any alterations in T cell morphology that occur upon contact with ICAM-1. In the presence of Mg^{2+}/EGTA, the T cells adhere to ICAM-1, and, by 45 seconds, they extend membrane projections that appear to govern the subsequent polarization of the T cell (Fig. 3; see Movie 1, available at jcs.biologists.org/supplemental). Between 90-120 seconds, T cell polarization becomes evident in that a ruffling leading edge dominates and the opposing edge contracts to form the trailing edge. By 150 seconds, the T cell becomes motile, indicating that the migratory machinery is fully engaged. A common feature of T cell migration in the absence of a chemotactic gradient is a frequent change in direction (see Movie 1 and Fig. 4D). In contrast, in the absence of Mg^{2+}/EGTA, T cells plated on ICAM-1 were non-attached (Fig. 4A), and Mg^{2+}/EGTA-treated T cells were similarly non-attached in the absence of ICAM-1 (BSA only) (data not shown). Thus attachment of T cells to ICAM-1 causes a signal that initiates polarization followed by migration.

A role for MLCK in T cell migration on ICAM-1

Because our data suggested involvement of MLCK in T cell attachment, we investigated its possible role in T cell migration on ICAM-1. When T cells made contact with ICAM-1 in the presence of Mg^{2+}/EGTA, attachment, polarization and migration occurred (Fig. 4B). These activities did not happen when Mg^{2+}/EGTA was omitted (Fig. 4A) and were also

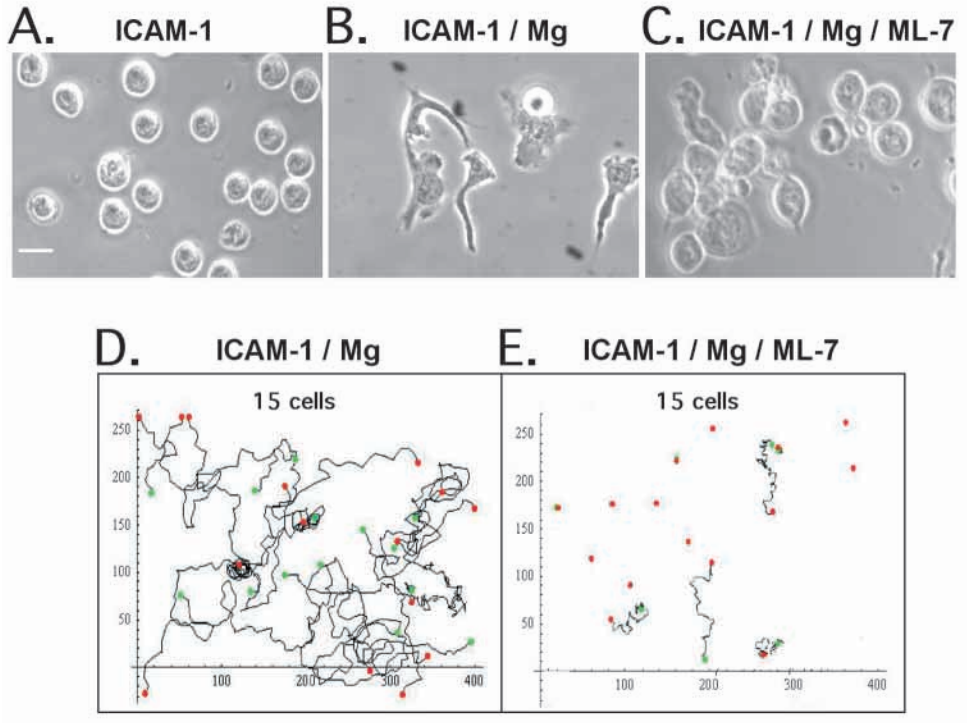

Fig. 4. Effect of inhibiting MLCK activity on T cell attachment and migration on ICAM-1. Phase images of T cells on (A) ICAM-1, (B) ICAM-1 in the presence of Mg^{2+}/EGTA, (C) pre-incubated with 20 μM ML-7 and plated onto ICAM-1 with Mg^{2+}/EGTA. Bar, 10 μm. Motility and migration as determined by time lapse microscopy (scale in μm). (D) T cells on ICAM-1 in the presence of Mg^{2+}/ EGTA (average speed=10.3 μm/minute; scale in μm). (E) T cells plated onto ICAM-1 in Mg^{2+}/EGTA and allowed to migrate for 20 minutes followed by the addition of 20 μM ML-7 for 70 minutes (average speed=0.71 μm/minute). Green and red dots represent the starting and stopping positions of each individual T cell.

prevented by preincubation with the MLCK inhibitor, ML-7 (Fig. 4C).

To test the effects of ML-7 on cell migration, T cells were allowed to migrate on ICAM-1 for 30 minutes and then tracked for an additional 70 minutes. Tracking individual cells showed that they followed a random course of migration with an average speed of 10.3±0.1 μm/minute (Fig. 4D). Addition of ML-7 resulted in the average speed decreasing to 0.71±0.03 μm/minute. This showed that blocking MLCK activity prevented T cell migration (Fig. 4E). To investigate the mechanism of the MLCK inhibition in more detail, the behavior of migrating T cells was followed by time lapse microscopy from the time of exposure to ML-7. In the presence of 20 μM ML-7, lamellar extension ceased within 1 minute and

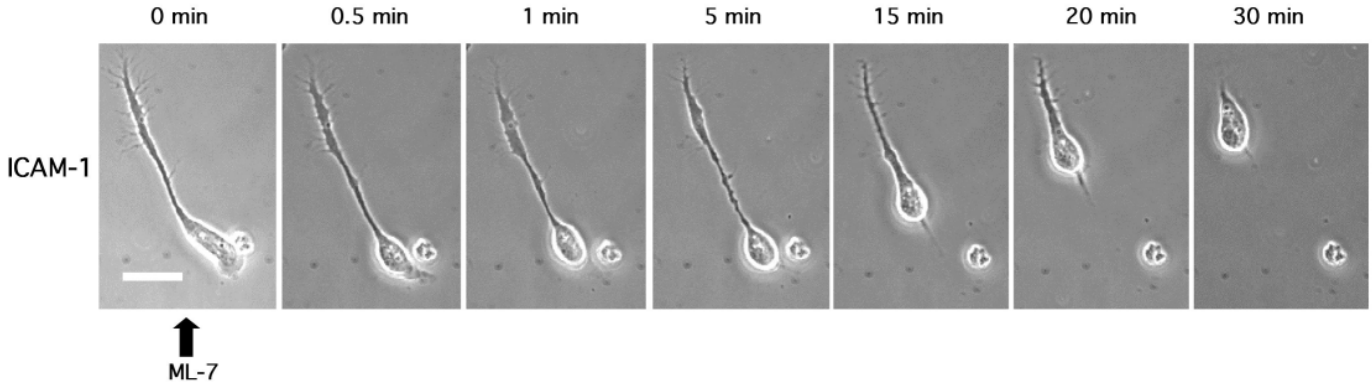

Fig. 5. Time lapse analysis of the effect of MLCK inhibition on morphology of the migrating T cell. ML-7 at a final concentration of 20 μM was added to T cells polarized on ICAM-1 in the presence of Mg^{2+}/EGTA, and the morphological response recorded by time lapse microscopy over 30 minutes. Bar, 10 μm.

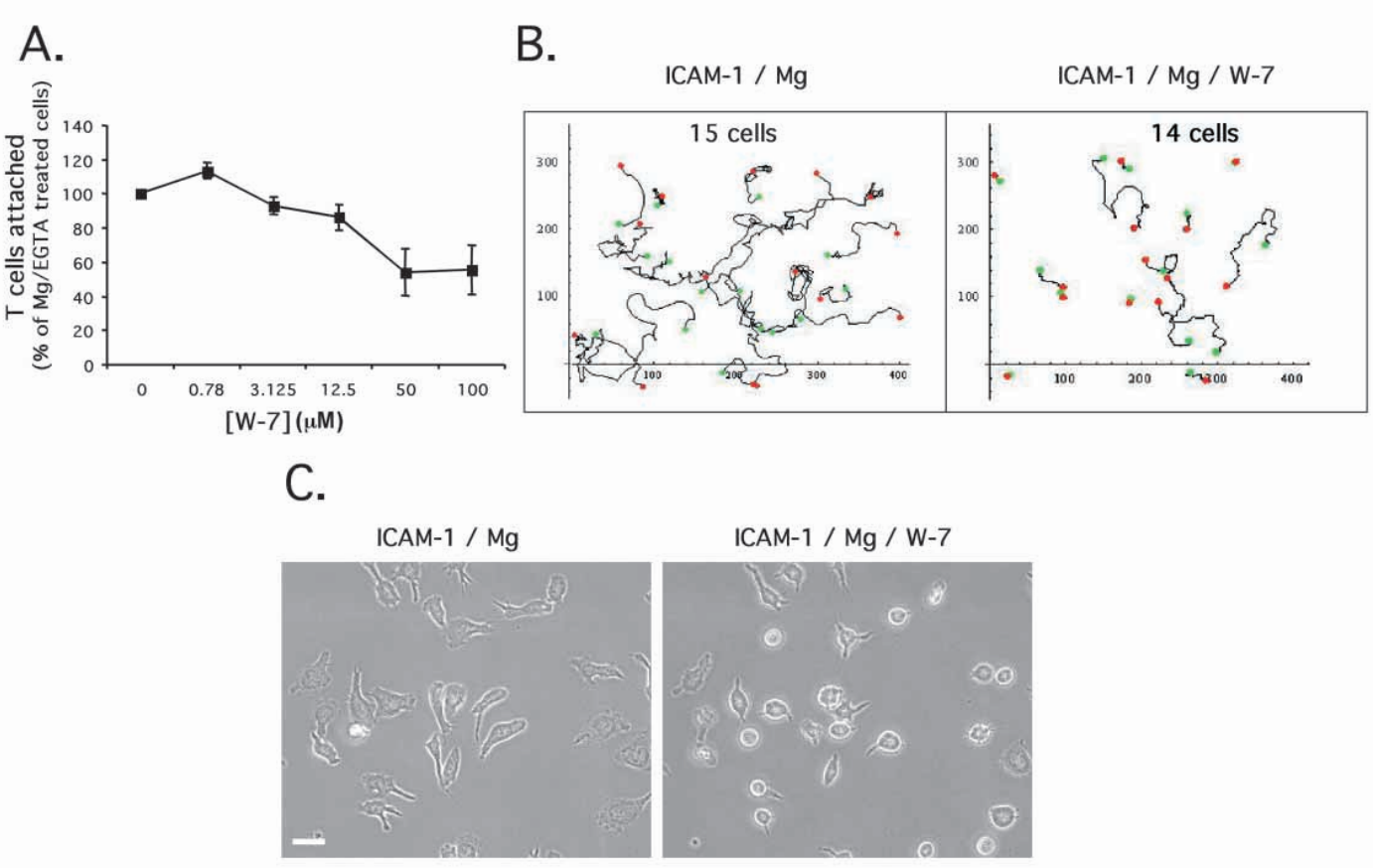

Fig. 6. Effect of inhibiting CaM activity on T cell attachment and migration on ICAM-1. (A) Proportion of T cells in presence of Mg^{2+}/EGTA bound to ICAM-1 over an increasing dose range of CaM inhibitor, W-7 (*n*=4). (B) Motility and migration as determined by time lapse microscopy (scale in μm). As in Fig. 4, Mg^{2+}/EGTA-stimulated T cells were plated onto ICAM-1 minus or plus pre-incubation with 50 μM W-7 and allowed to migrate for 30 minutes (average speed of 7.85±0.15 versus 1.53±0.05 μm/minute). Green and red dots represent the starting and stopping positions of each individual T cell. (C) Phase images of Mg^{2+}/EGTA-stimulated T cells plated onto ICAM-1 and allowed to migrate for 30 minutes followed by the addition of 50 μM W-7 for 10 minutes. Bar, 20 μm.

the main cell body gradually retracted and collapsed back towards the trailing edge (Fig. 5; see Movie 2, available at jcs.biologists.org/supplemental). These results provide the first evidence that MLCK has a key role at the leading edge of the migrating T cell.

A role for CaM in T cell migration

A known regulator of MLCK activity is CaM, which activates MLCK by binding to its regulatory domain (Lukas et al., 1986). The CaM inhibitor W-7 blocks T cell attachment to ICAM-1 with maximum effect at 50-100 μM (Fig. 6A). Microscopic examination showed that T cells, in contact with ICAM-1 and Mg^{2+}/EGTA, attached and polarized, but following preincubation with W-7, the cells were rounded and failed to polarize (data not shown). To assess the effect on cell migration, T cells were tracked over 60 minutes after exposure to W-7. As previously noted, individual cells displayed a random course of migration with an average speed of 7.94±0.15 μm/minutes, but following preincubation with 50 μM W-7, the average speed decreased to 1.53±0.15 μm/minutes (Fig. 6B). To assess, in more detail, where CaM might be acting in the migratory process, T cells were allowed to migrate on ICAM-1 for 20 minutes prior to exposure to 50 μM W-7. After treatment with W-7, lamellar extension rapidly ceased, and the main cell body gradually retracted, mirroring the effects of MLCK inhibition **(**Fig. 6C; Movie 3, available at jcs.biologists.org/supplemental).

T cell migration on ICAM-1: a role for ROCK in de-adhesion

Inhibition of ROCK with Y-27632 had no effect on T cell attachment to ICAM-1 (Fig. 1B). However, when migrating T cells were treated with 10 μM Y-27632, the trailing edge of the T cells was substantially elongated compared with control T cells (Fig. 7A). Incubation of the T cells with C3 exoenzyme mirrored this effect, indicating a role for RhoA as the activator of ROCK (Fig. 7B, and supplementary figure 1, available at jcs.biologists.org/supplemental).

Tail elongation could potentially occur via an extensive protrusion from the cell or, alternatively, by a failure to detach the trailing edge as the cell moved forward. To analyze the effect of ROCK inhibition at the single cell level, we again used

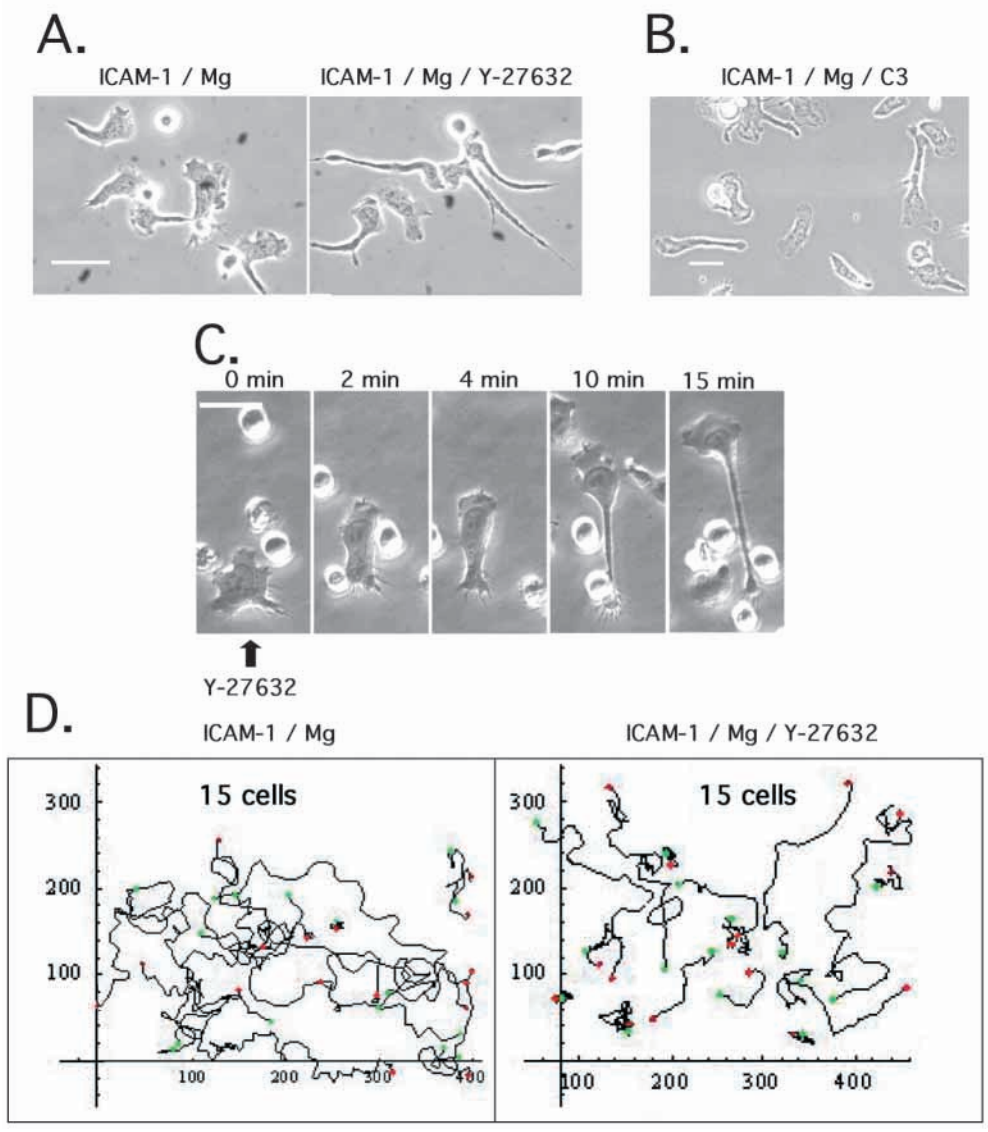

Fig. 7. Effect of inhibiting ROCK activity on T cell attachment and migration on ICAM-1. Phase images of Mg^{2+}/EGTA-stimulated T cells after 20 minutes of migration. (A) On ICAM-1 or pre-incubated with 10 μM Y-27632. (B) T cells, pre-incubated with C3 exoenzyme overnight at 37°C prior to plating on ICAM-1. (C) T cells were allowed to adhere to ICAM-1 in presence of Mg^{2+}/EGTA for 20 minutes followed by the addition of 10 μM Y-27632. The morphological effects were recorded by time lapse microscopy over 15 minutes (bar, 20 μm). (D) T cells on ICAM-1 in the presence of Mg^{2+}/EGTA (average speed=12.6±0.22 μm/minute). T cells were allowed to adhere for 20 minutes followed by the addition of 10 μM Y-27632 for 70 minutes (average speed=4.81±0.13 μm/minute; scale in μm). Green and red dots represent the starting and stopping positions of each individual T cell.

time lapse microscopy to visualize the cells. T cells were allowed to attach and migrate for 20 minutes on ICAM-1 before Y-27632 was added. Observation of T cells following Y-27632 treatment revealed that elongation occurred because the leading edge continued to be highly motile, whereas movement ceased at the trailing edge (Fig. 7C, Movie 4, available at jcs.biologists.org/suplemental). This was attributable to the tail remaining firmly anchored to ICAM-1. This lack of detachment had a negative effect on T cell migration, resulting in an average decrease in cell speed from 12.60±0.22 to 4.81±0.13 μm/minute (Fig. 7D). Therefore, inhibition of ROCK did not prevent activity at the leading edge of the T cell, but prevented detachment at the trailing edge necessary for cellular translocation.

Distinct roles of the MLCK and ROCK as assessed by cell spreading

To gain further insight into the roles of MLCK and ROCK in T cell migration, we examined their contribution to the spreading of T cells on ICAM-1. We tested the effect of the inhibitors by quantifying both area of cell spread and also the length of the migrating T cell. There was a reduction in area of cell spread of T cells treated with ML-7 (21.1%) and W-7 (22.8%) on ICAM-1 compared with control migrating T cells (Fig. 8A). This reduction was similar to that of non-spreading T cells on control BSA substrate (29.4%). There was also a loss of cell length induced by ML-7 (35.7%) and W-7 (26.8%) as expected with the loss of cell spreading and retraction to a rounded shape (Fig. 8B).

In contrast, ROCK inhibition produced no significant alteration in cell spread area compared with the control T cells (Fig. 8A). However, the Y-27632-treated T cells showed an average overall increase in cell length of 40% compared with untreated T cells (Fig. 8B**)**. RhoA inhibition increases cell length in a comparable fashion to ROCK inhibition (Fig. 8B**)**.

Subcellular localization of actin, myosin and the two kinases, MLCK and ROCK

The findings so far have indicated that the kinases MLCK and ROCK are important for forward propulsion and rear detachment, respectively, during LFA-1-mediated T cell migration on ICAM-1. It was, therefore, of interest to localize the two kinases in the migrating T cell and to compare their distribution with that of F-actin and myosin II. Immunofluorescence revealed that the F-actin filaments were concentrated predominantly in the lamellipodial projections at the leading edge of the T cell with much lower staining in the main body of the cell (Fig. 9). MLCK was most concentrated at the leading edge of the T cells overlapping with F-actin positive lamellipodial extensions and was not detectable at the same level elsewhere (Fig. 9A). In contrast, ROCK staining was more generally distributed in the tail region (Fig. 9B). Thus MLCK and ROCK are spatially separated in the cell.

Given that MLCK and ROCK show different distribution patterns, we next investigated the expression pattern of myosin II. There was a high concentration of myosin at the leading edge of the cell where the pattern of staining ranged from either lining the F-actin-positive extensions (Fig. 9C) or overlapping with the F-actin-positive lamelli (data not shown). Myosin was also expressed in the tail region of the polarized T cell where F actin was also localized. In summary, myosin was strongly detected in the leading edge and tail of the T cell, corresponding to the locations enriched in MLCK and ROCK respectively.

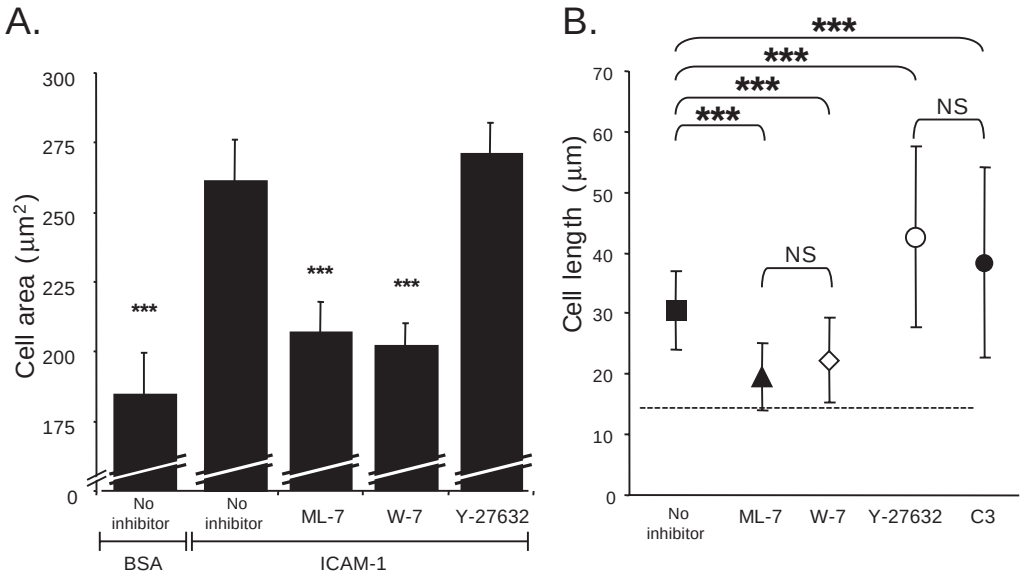

Fig. 8. Effect of MLCK, CaM and ROCK inhibitors on cell spreading and morphology. (A) Mg^{2+}/EGTA-stimulated T cells were allowed to migrate on ICAM-1 or BSA for 20 minutes in the presence of either ML-7 (25 μM), W-7 (50 μM) or Y-27632 (20 μM) prior to fixation, permeabilization and staining for F-actin (*n*=6). Cell area was recorded by a LSC (6000 cells per cover slip). (B) T cell length was measured after incubation with either ML-7 (25 μM), W-7 (50 μM), Y-27632 (20 μM) or C3 exoenzyme (20 μg/ml) (*n*=18-34). All measurements were taken after the T cells were allowed to migrate for 20 minutes on ICAM-1 in the presence of Mg^{2+}/EGTA. The dotted line represents the average diameter of T cells in suspension (included as a reference point). All results are expressed as an mean±s.d. $P<0.01$(***).

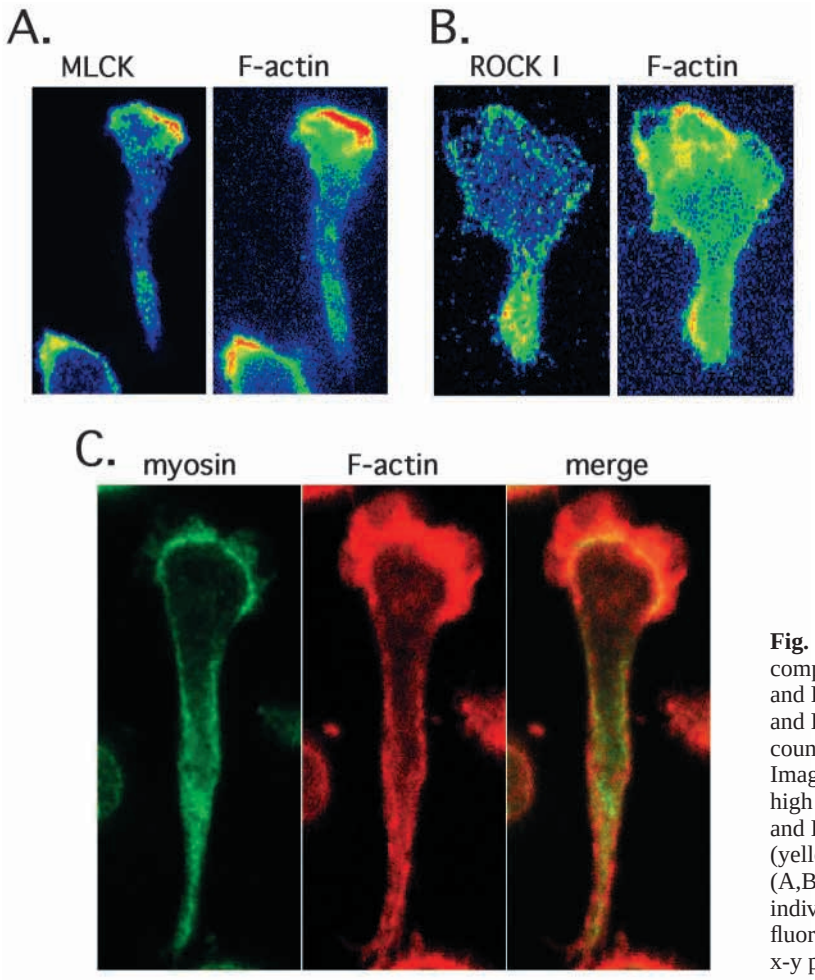

Fig. 9. Subcellular localization of MLCK, ROCK and myosin compared to actin in T cells migrating on ICAM-1. MLCK (A) and ROCK (B) were detected with mAbs specific for MLCK and ROCK I, followed by Alexa 488-goat anti-mouse IgG and counter-stained with Alexa 546-phalloidin to visualize F-actin. Images are displayed as gradient maps where red represents high and blue low fluorescence intensity. (C) Myosin (green) and F-actin (red) were merged to determine colocalization (yellow) within an Mg^{2+}/EGTA-stimulated T cell on ICAM-1. (A,B) Images represent projections onto the x-y plane of all individual optical sections taken along the z-axis using maximal fluorescence values. Image C represents a single section in the x-y plane.

MLCK and ROCK both affect T cell migration but by different routes

Inhibiting either MLCK (with ML-7 or indirectly through the CaM inhibitor,W-7) or ROCK (Y-27632) reduced the speed of T cell migration. An average speed of 10.30±1.74 μm/minute was reduced to 0.71±0.03 (ML-7), 1.53±0.15 (W-7) or 4.81±0.13 (Y-27632) μm/minute (Fig. 10A). In order to determine how general were the described inhibitory effects of ROCK and MLCK, we quantified the proportion of attached cells within the T cell population that were actively migrating, displaying lamellar protrusion and, finally, displaying firmly anchored tails. In a population of untreated T cells, 63% were actively migrating, whereas 37% polarized but failed to migrate (Fig. 10B). All cells exhibited active lamella. In the presence of Y-27632, the proportion of migrating cells was reduced with a concomitant increase in the number of cells with anchored tails. Importantly, as with untreated T cells, these cells exhibited lamellar protrusion, providing further evidence that the activity of ROCK was restricted to the trailing edge. However, when MLCK (or CaM) was blocked, the percentage of cells that were migrating dropped to <10% of the total, and this was accompanied by a loss of lamellar extension activity.

When both ML-7 and Y-27632 were co-incubated with the T cells, the ML-7 effect prevailed with no moderating effect of Y-27632. (see supplementary figure 1, available at jcs.biologists.org/supplemental). These data suggest that MLCK function at the leading edge dominates the ROCK-generated events at the trailing edge in terms of T cell migration. Evidence for the independent control of T cell migration by MLCK and ROCK was demonstrated by co-incubating T cells with their respective inhibitors (Movie 5, available at jcs.biologists.org/supplemental). T cells were first exposed to Y-27632 and displayed the attached tail phenotype. Subsequently, following MLCK inhibition, it was observed that the collapse of the leading edge did not affect the firmly anchored tail. This further demonstrates that compartmentized signaling events are required for the attachment and detachment of the migrating T cell.

Discussion

A major finding of this study is that T cell migration can be initiated and sustained solely through the signaling pathway(s) generated by LFA-1 binding to ICAM-1. Previously, we have demonstrated that LFA-1-mediated adhesion on ICAM-1 causes reorganization of the actin cytoskeleton (Porter et al., 2002). We extend this data by showing that T cells in the presence of Mg^{2+} migrate at a rate of ~10 μm/minute on ICAM-1, and this migration is dependent upon kinases, MLCK and ROCK.

MLCK is located at the leading edge of the T cell where the

A.

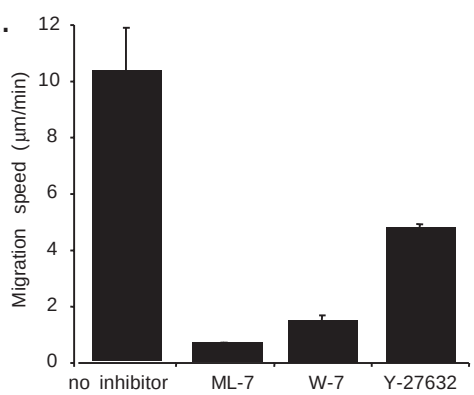

B.

	cell migration	lamellar protrusion	tail anchored
no inhibitor	63 %	100 %	37 %
ML-7	8 %	20 %	NA
W-7	0 %	8 %	NA
Y-27632	31 %	100 %	69 %

Fig. 10. Effect of MLCK and ROCK inhibitors on migration of the T cell population. (A) Average speed of Mg^{2+}/EGTA-stimulated T cells on ICAM-1 in the presence of inhibitors 25 μM ML-7, 50 μM W-7, 20 μM Y-27632 (all n=15) or no inhibitor (n=55). (B) The T cells were plated on ICAM-1 in the presence of Mg^{2+}/EGTA and allowed to migrate for 20 minutes. Inhibitor treatment was initiated and the T cells were scored after a further 10 minutes. 'Lamellar protrusion' describes membrane ruffling at either the leading edge or, in the case of stationary cells, around the cell circumference. 'Tail anchored' describes polarized cells that failed to translocate a full cell length. n=50-70 per treatment group.

lamellipodia are in a continual and rapid process of protruding and retracting as the cell moves forward. MLCK inhibition prior to T cell contact with ICAM-1 greatly reduces cellular attachment, showing that it has a direct role in this activity. Insight into this process was obtained when MLCK activity is inhibited after cell migration is underway. In this situation, lamellipodial extensions collapse and the T cell retracts towards the trailing edge. This is further confirmed by the reduction in cell spreading to levels similar to the non-motile T cells. These observations indicate that MLCK has an active role at the front of the migrating T cell in extending the leading edge and permitting new attachments required for forward movement. A role for MLCK in cell division and migration has also been described for PTK2 kangaroo rat epithelial cells (Chew et al., 2002).

The upstream activator of MLCK is CaM in many cell types (Lukas et al., 1986). In this study, the effect of inhibiting MLCK in T cells is mirrored by inhibiting the activity of CaM. Many downstream effectors are activated by CaM, and it is therefore of interest that MLCK appears to be its predominant target in the migrating T cell. The only recognized substrate of MLCK is MLC, which is phosphorylated on Thr18 Ser19, thereby activating myosin ATPase activity (reviewed in Bresnick, 1999). There is also evidence in smooth muscle cells that the actin-bundling activity of MLCK, rather than the kinase activity, is dominant in membrane ruffling (Kishi et al., 2000; Ye et al., 1999). The inhibitor ML-7 and the MLCK auto-inhibitory peptide used in this study both target the kinase domain and block catalytic activity of MLCK (Saitoh et al., 1987; Tanaka et al., 1995). The fact that these agents prevent T cell attachment and migration provides evidence that it is the kinase activity of MLCK that is paramount.

A number of forms of human MLCK have been identified, of which the most common are a 'small' ~130-150 kDa smooth muscle form and a 'large' higher molecular weight non-smooth muscle form of ~220 kDa (Blue et al., 2002; Kamm and Stull, 2001). T cells contain a ~140 kDa MLCK, which equates to the small form and an intermediate molecular weight form of ~166 kDa. No band could be detected in T cells that represented the large 220 kDa MLCK. In comparison with murine lung cells and other cell lines (data not shown), MLCK appears to be expressed in low abundance in human T cells. Four other variants of the MLCK protein have been described previously (Lazar and Garcia, 1999) and, from the chicken genomic sequence, the identification of canonical splice consensus sites in each of the 31 exons raises the possibility that more forms exist (Birukov et al., 1998).

In fibroblasts, the large form of MLCK contains five rather than the three actin-binding motifs found in the small form (Kudryashov et al., 1999; Smith et al., 2002; Smith et al., 1999). The resulting higher affinity for actin (Smith et al., 2002) is suggested as an explanation for the targeting of the large form of MLCK to actin stress fibers and to the cleavage furrow of dividing cells (Poperechnaya et al., 2000). In our study we show that there is a high degree of colocalization of MLCK with the dense networks of F-actin comprising the dynamic T cell lamelli. It is tempting to speculate that the 166 kDa MLCK, which we identify here, also contains extra actin-binding motifs, strengthening binding to F-actin. Further characterization of T cell MLCK will be needed to test this hypothesis.

ROCK, like MLCK, is a major serine/threonine kinase that phosphorylates MLC, leading to activation of myosin ATPase activity (Amano et al., 1996). The negligible effect on T cell attachment assays of inhibiting ROCK and its activator RhoA (supplementary figure 1, available at jcs.biologists.org/supplemental) suggested that they play no major role in the signaling events responsible for T cell attachment to ICAM-1. However, video microscopy revealed a dramatic effect of ROCK inhibition on the migratory ability of T cells. Blocking ROCK resulted in the trailing edge of the T cell remaining firmly adhered to ICAM-1, whereas the leading edge continued to progress forward. These two opposing processes resulted in the generation of an artificially elongated cell.

The failure of tail detachment when ROCK (and RhoA) activity is inhibited could occur because of an increased number of LFA-1-mediated attachments rather than an increase in stability of the pre-existing attachments. However, as both cell attachment and cell spreading analyses provide no evidence for an increase in attachments, the most likely explanation is that ROCK inhibition increases the stability of

pre-existing attachments, leading to the failure to detach the trailing edge in coordination with the forward movement at the front end of the cell. Alternatively, by causing MLC phosphorylation and activating the myosin motor, ROCK may enhance the contractile force of the trailing edge, thereby overcoming the binding strength of the LFA-1/ICAM-1 adhesions. ROCK also contributes to phosphorylated MLC stability via inhibition of myosin phosphatase (Kimura et al., 1996). Additionally, ROCK can phosphorylate other substrates such as moesin, adducin, intermediate filament proteins, LIM kinase and the NaH exchanger (Fukata et al., 1998; Fukata et al., 1999; Kosako et al., 1997; Sumi et al., 2001; Tominaga et al., 1998). ROCK may therefore promote de-adhesion by a pathway not involving myosin. However preliminary evidence indicates that inhibition of ROCK activity by Y-27632 decreases the phosphorylation of MLC on Ser 19, which pinpoints MLC as the relevant downstream target of ROCK in migrating T cells (data not shown). This same finding also makes it less likely that the effects of Y-27632 are attributable to inhibition of the Rho/Rac binding kinase, PRK2, as has recently been described (Davies et al., 2000).

The upstream activator of ROCK is RhoA in other cell types (Ridley, 2001), and we show here that the RhoA inhibitor C3 exoenzyme mimics the effects of ROCK inhibition in causing tail elongation in migrating T cells. Other evidence that RhoA is active in T cells comes from the analysis of RhoA activity using an in vitro kinase pull-down assay with Rhotekin (Ren et al., 1999), which showed a time-dependent increase in RhoA activity that was dependent upon contact with ICAM-1 (data not shown). A similar role for Rho A and ROCK has been described for de-adhesion of the tail end of migrating eosinophils (Alblas et al., 2001) and monocytes (Worthylake et al., 2001). Thus ROCK appears to be required for detachment of the trailing edge, allowing forward migration of several types of leukocytes.

Our data show that there is spatial regulation of MLCK and ROCK activity, initiated by LFA-1 binding to ICAM-1, with MLCK operating at the leading edge and ROCK found in highest concentration in the body and trailing edge of the migrating T cell. The distribution of these two kinases suggests that there are two compartments with distinct functions operating in the migrating T cell. Separation of these two kinases has been observed previously in murine 3T3 (Totsukawa et al., 2000) and human fibroblasts (Katoh et al., 2001). In these studies, ROCK activity was associated with stress fibers in the center of cells, whereas MLCK was associated with peripheral cortical microfilaments. In contrast, when neutrophil migration was examined, blocking of both ROCK (Niggli, 1999) and MLCK (Eddy et al., 2000) caused delayed retraction of the tail end of the cell, suggesting they were both active in the same cellular compartment. Differences in migratory machinery may exist between even closely related cell types that are tailored to the role that migration performs in cellular function.

Separate control of MLCK and ROCK enables the front and rear of the cell to contribute in different ways to T cell migration. There are several speculations as to why these two kinases operate in different areas within a migrating T cell. MLCK phosphorylates MLC in vitro with a sixfold higher Km than ROCK (Amano et al., 1996). It may be that the rapid lamellar activity, which is associated with MLCK, requires a kinase with high Km, whereas the generalized contraction of the tail end of the migrating cells may be better effected by a slow acting kinase like ROCK. The dynamic lamellar movement at the leading edge may also benefit from myosin phosphatase activity that would be enhanced in a compartment of reduced ROCK activity. Coordination of the two compartments must lie farther upstream from the immediate activation of MLCK and ROCK by CaM and RhoA, respectively. In the BHK cell line there is a link between the GTPases Rac and RhoA in control of MLC phosphorylation, with Rac causing MLCK inactivation through PAK1-mediated phosphorylation, and RhoA causing ROCK activation (Sanders et al., 1999). How these activities are coordinated and whether similar pathways exist in primary T cells is not known.

Direct activation of LFA-1 followed by exposure to immobilized ICAM-1 is sufficient to cause T cells to attach, polarize and randomly migrate within 3 minutes. This migration is dependent on MLCK and ROCK, which control the activity of acto-myosin. Our in vitro analysis of T cell migration parallels a recent two-photon microscopic study showing randomly moving T cells in the lymph node with a speed of 11 μm/minute (Miller et al., 2003). These two techniques will provide a powerful combination to unravel the mechanisms involved in T cell migration. ICAM-1 is not only expressed in lymphoid tissue but is also rapidly induced in other tissues following inflammatory stimuli. This suggests that T cell migration is relevant not only in the lymphoid compartment but also in other tissues. LFA-1 has previously been associated with the acto-myosin transport involved in delivering receptors to the contact area or ‘synapse’ by which leukocytes contact target cells, implying that LFA-1 signaling also has a role in cell-cell contact events (Wulfing and Davis, 1998). In summary, LFA-1 is not just an adhesion receptor but also a signaling molecule that can direct acto-myosin-based T cell functions by its coordinated activation of MLCK and ROCK.

We are grateful to N. O’Reilly and D. Joshi, Protein and the Peptide Chemistry Laboratory for synthesizing the antennapedia peptides. We also thank C. Gray and D. Aubyn (Light Microscopy Laboratory) and D. Davies (Fluorescence Activated Cell Sorter Laboratory) for their help with the microscopy in this study. We thank our Leukocyte Adhesion Laboratory colleagues and Cancer Research UK colleague, M. Way for careful comments on the manuscript. M.B. was supported by an EMBO Fellowship and B.L. by Celltech R&D Ltd.

References

Alblas, J., Ulfman, L., Hordijk, P. and Koenderman, L. (2001). Activation of Rhoa and ROCK are essential for detachment of migrating leukocytes. *Mol. Biol. Cell* **12**, 2137-2145.

Amano, M., Ito, M., Kimura, K., Fukata, Y., Chihara, K., Nakano, T., Matsuura, Y. and Kaibuchi, K. (1996). Phosphorylation and activation of myosin by Rho-associated kinase (Rho- kinase). *J. Biol. Chem.* **271**, 20246-20249.

Berendt, A. R., McDowall, A., Craig, A. G., Bates, P. A., Sternberg, M. J., Marsh, K., Newbold, C. I. and Hogg, N. (1992). The binding site on ICAM-1 for Plasmodium falciparum-infected erythrocytes overlaps, but is distinct from, the LFA-1 binding site. *Cell* **68**, 71-81.

Birukov, K. G., Schavocky, J. P., Shirinsky, V. P., Chibalina, M. V., van Eldik, L. J. and Watterson, D. M. (1998). Organization of the genetic locus for chicken myosin light chain kinase is complex: multiple proteins are encoded and exhibit differential expression and localization. *J. Cell Biochem.* **70**, 402-413.

Blue, E. K., Goeckeler, Z. M., Jin, Y., Hou, L., Dixon, S. A., Herring, B.

P., Wysolmerski, R. B. and Gallagher, P. J. (2002). 220- and 130-kDa MLCKs have distinct tissue distributions and intracellular localization patterns. *Am. J. Physiol. Cell Physiol.* **282**, C451-C460.
Bresnick, A. R. (1999). Molecular mechanisms of nonmuscle myosin-II regulation. *Curr. Opin. Cell Biol.* **11**, 26-33.
Chew, T.-L., Wolf, W. A., Gallagher, P. J., Matsumura, F. and Chisholm, R. L. (2002). A flourescent resonant energy transfer-based biosensor reveals transient and regional myosin light chain kinase activation in lamella and cleavage furrows. *J. Cell Biol.* **156**, 543-553.
Darzynkiewicz, Z., Bedner, E., Li, X., Gorczyca, W. and Melamed, M. R. (1999). Laser-scanning cytometry: a new instrumentation with many applications. *Exp. Cell Res.* **249**, 1-12.
Davies, S. P., Reddy, H., Caivano, M. and Cohen, P. (2000). Specificity and mechanism of action of commonly used protein kinase inhibitors. *Biochem. J.* **351**, 95-105.
Dransfield, I., Cabanas, C., Craig, A. and Hogg, N. (1992). Divalent cation regulation of the function of the leukocyte integrin LFA-1. *J. Cell Biol.* **116**, 219-226.
Eddy, R. J., Pierini, L. M., Matsumura, F. and Maxfield, F. R. (2000). Ca^{2+}-dependent myosin II activation is required for uropod retraction during neutrophil migration. *J. Cell Sci.* **113**, 1287-1298.
Friedl, P. and Gunzer, M. (2001). Interaction of T cells with APCs: the serial encounter model. *Trends Immunol.* **22**, 187-191.
Fukata, Y., Kimura, K., Oshiro, N., Saya, H., Matsuura, Y. and Kaibuchi, K. (1998). Association of the myosin-binding subunit of myosin phosphatase and moesin: dual regulation of moesin phosphorylation by Rho-associated kinase and myosin phosphatase. *J. Cell Biol.* **141**, 409-418.
Fukata, Y., Oshiro, N., Kinoshita, N., Kawano, Y., Matsuoka, Y., Bennett, V., Matsuura, Y. and Kaibuchi, K. (1999). Phosphorylation of adducin by Rho-kinase plays a crucial role in cell motility. *J. Cell Biol.* **145**, 347-361.
Horwitz, A. R. and Parsons, J. T. (1999). Cell migration–movin' on. *Science* **286**, 1102-1103.
Ishizaki, T., Maekawa, M., Fujisawa, K., Okawa, K., Iwamatsu, A., Fujita, A., Watanabe, N., Saito, Y., Kakizuka, A., Morii, N. et al. (1996). The small GTP-binding protein Rho binds to and activates a 160 kDa Ser/Thr protein kinase homologous to myotonic dystrophy kinase. *EMBO J.* **15**, 1885-1893.
Kamm, K. E. and Stull, J. T. (2001). Dedicated myosin light chain kinases with diverse cellular functions. *J. Biol. Chem.* **276**, 4527-4530.
Katoh, K., Kano, Y., Amano, M., Kaibuchi, K. and Fujiwara, K. (2001). Stress fiber organization regulated by MLCK and Rho-kinase in cultured human fibroblasts. *Am. J. Physiol. Cell Physiol.* **280**, C1669-C1679.
Kimura, K., Ito, M., Amano, M., Chihara, K., Fukata, Y., Nakafuku, M., Yamamori, B., Feng, J., Nakano, T., Okawa, K. et al. (1996). Regulation of myosin phosphatase by Rho and Rho-associated kinase (Rho-kinase). *Science* **273**, 245-248.
Kishi, H., Mikawa, T., Seto, M., Sasaki, Y., Kanayasu-Toyoda, T., Yamaguchi, T., Imamura, M., Ito, M., Karaki, H., Bao, J. et al. (2000). Stable transfectants of smooth muscle cell line lacking the expression of myosin light chain kinase and their characterization with respect to the actomyosin system. *J. Biol. Chem.* **275**, 1414-1420.
Kosako, H., Amano, M., Yanagida, M., Tanabe, K., Nishi, Y., Kaibuchi, K. and Inagaki, M. (1997). Phosphorylation of glial fibrillary acidic protein at the same sites by cleavage furrow kinase and Rho-associated kinase. *J. Biol. Chem.* **272**, 10333-10336.
Kudryashov, D. S., Chibalina, M. V., Birukov, K. G., Lukas, T. J., Sellers, J. R., van Eldik, L. J., Watterson, D. M. and Shirinsky, V. P. (1999). Unique sequence of a high molecular weight myosin light chain kinase is involved in interaction with actin cytoskeleton. *FEBS Lett.* **463**, 67-71.
Lazar, V. and Garcia, J. G. (1999). A single human myosin light chain kinase gene (MLCK; MYLK). *Genomics* **57**, 256-267.
Lukas, T. J., Burgess, W. H., Prendergast, F. G., Lau, W. and Martin Watterson, D. (1986). Calmodulin binding domains: characterization of a phosphorylation and calmodulin binding site from myosin light chain kinase. *Biochemistry* **25**, 1458-1464.
Miller, M. J., Wei, S. H., Cahalan, M. D. and Parker, I. (2003). Autonomous T cell trafficking examined in vivo with intravital two-photon microscopy. *Proc. Natl. Acad. Sci. USA* **100**, 2604-2609.
Niggli, V. (1999). Rho-kinase in human neutrophils: a role in signalling for myosin light chain phosphorylation and cell migration. *FEBS Lett.* **445**, 69-72.
Poperechnaya, A., Varlamova, O., Lin, P. J., Stull, J. T. and Bresnick, A. R. (2000). Localization and activity of myosin light chain kinase isoforms during the cell cycle. *J. Cell Biol.* **151**, 697-708.
Porter, J. C. and Hogg, N. (1997). Integrin cross talk: activation of lymphocyte function-associated antigen-1 on human T cells alters alpha4beta1- and alpha5beta1-mediated function. *J. Cell Biol.* **138**, 1437-1447.
Porter, J. C., Bracke, M., Smith, A., Davies, D. and Hogg, N. (2002). Signaling through integrin LFA-1 leads to filamentous actin polymerization and remodeling, resulting in enhanced T cell adhesion. *J. Immunol.* **168**, 6330-6335.
Ren, X. D., Kiosses, W. B. and Schwartz, M. A. (1999). Regulation of the small GTP-binding protein Rho by cell adhesion and the cytoskeleton. *EMBO J.* **18**, 578-585.
Ridley, A. J. (2001). Rho family proteins: coordinating cell responses. *Trends Cell Biol.* **11**, 471-477.
Saitoh, M., Ishikawa, T., Matsushima, S., Naka, M. and Hidaka, H. (1987). Selective inhibition of catalytic activity of smooth muscle myosin light chain kinase. *J. Biol. Chem.* **262**, 7796-7801.
Sanders, L. C., Matsumura, F., Bokoch, G. M. and de Lanerolle, P. (1999). Inhibition of myosin light chain kinase by p21-activated kinase. *Science* **283**, 2083-2085.
Serrador, J. M., Nieto, M. and Sanchez-Madrid, F. (1999). Cytoskeletal rearrangement during migration and activation of T lymphocytes. *Trends Cell Biol.* **9**, 228-233.
Smith, L., Parizi-Robinson, M., Zhu, M. S., Zhi, G., Fukui, R., Kamm, K. E. and Stull, J. T. (2002). Properties of long Myosin light chain kinase binding to f-actin in vitro and in vivo. *J. Biol. Chem.* **277**, 35597-35604.
Smith, L., Su, X., Lin, P., Zhi, G. and Stull, J. T. (1999). Identification of a novel actin binding motif in smooth muscle myosin light chain kinase. *J. Biol. Chem.* **274**, 29433-29438.
Stewart, M. and Hogg, N. (1996). Regulation of leukocyte integrin function: affinity vs. avidity. *J. Cell Biochem.* **61**, 554-561.
Sumi, T., Matsumoto, K. and Nakamura, T. (2001). Specific activation of LIM kinase 2 via phosphorylation of threonine 505 by ROCK, a Rho-dependent protein kinase. *J. Biol. Chem.* **276**, 670-676.
Tanaka, M., Ikebe, R., Matsuura, M. and Ikebe, M. (1995). Pseudosubstrate sequence may not be critical for autoinhibition of smooth muscle myosin light chain kinase. *EMBO J.* **14**, 2839-2846.
Tominaga, T., Ishizaki, T., Narumiya, S. and Barber, D. L. (1998). p160ROCK mediates RhoA activation of Na-H exchange. *EMBO J.* **17**, 4712-4722.
Totsukawa, G., Yamakita, Y., Yamashiro, S., Hartshorne, D. J., Sasaki, Y. and Matsumura, F. (2000). Distinct roles of ROCK (Rho-kinase) and MLCK in spatial regulation of MLC phosphorylation for assembly of stress fibers and focal adhesions in 3T3 fibroblasts. *J. Cell Biol.* **150**, 797-806.
van Kooyk, Y. and Figdor, C. G. (2000). Avidity regulation of integrins: the driving force in leukocyte adhesion. *Curr. Opin. Cell Biol.* **12**, 542-547.
Volkov, Y., Long, A., McGrath, S., Ni Eidhin, D. and Kelleher, D. (2001). Crucial importance of PKC-beta(I) in LFA-1-mediated locomotion of activated T cells. *Nat. Immunol.* **2**, 508-514.
Walker, J. W., Gilbert, S. H., Drummond, R. M., Yamada, M., Sreekumar, R., Carraway, R. E., Ikebe, M. and Fay, F. S. (1998). Signaling pathways underlying eosinophil cell motility revealed by using caged peptides. *Proc. Natl. Acad. Sci. USA* **95**, 1568-1573.
Worthylake, R. A. and Burridge, K. (2001). Leukocyte transendothelial migration: orchestrating the underlying molecular machinery. *Curr. Opin. Cell Biol.* **13**, 569-577.
Worthylake, R. A., Lemoine, S., Watson, J. M. and Burridge, K. (2001). RhoA is required for monocyte tail retraction during transendothelial migration. *J. Cell Biol.* **154**, 147-160.
Wulfing, C. and Davis, M. M. (1998). A receptor/cytoskeletal movement triggered by costimulation during T cell activation. *Science* **282**, 2266-2269.
Ye, L. H., Kishi, H., Nakamura, A., Okagaki, T., Tanaka, T., Oiwa, K. and Kohama, K. (1999). Myosin light-chain kinase of smooth muscle stimulates myosin ATPase activity without phosphorylating myosin light chain. *Proc. Natl. Acad. Sci. USA* **96**, 6666-6671.